Eur. Phys. J. C (2017) 77:597
DOI 10.1140/epjc/s10052-017-5120-2

THE EUROPEAN PHYSICAL JOURNAL C

Regular Article - Theoretical Physics

Study of color-octet matrix elements through J/ψ production in e^+e^- annihilation

Yi-Jie Li[1], **Guang-Zhi Xu**[1], **Pan-Pan Zhang**[1], **Yu-Jie Zhang**[2,3,a], **Kui-Yong Liu**[1,b]

[1] Department of Physics, Liaoning University, Shenyang 110036, China
[2] School of Physics, Beihang University, Beijing 100191, China
[3] CAS Center for Excellence in Particle Physics, Beijing 100049, China

Received: 25 January 2017 / Accepted: 24 July 2017 / Published online: 9 September 2017

Abstract In this paper, the color-octet long distance matrix elements are studied through the inclusive J/ψ production in e^+e^- annihilation within the framework of non-relativistic QCD factorization. The calculations are up-to next-to-leading order with the radiative and relativistic corrections in the energy region of the B-factory and the near-threshold region of 4.6−5.6 GeV. A constraint of the long distance matrix elements ($\langle{}^1S_0^8\rangle$, $\langle{}^3P_0^8\rangle$) is obtained. Through our estimation, the P-wave color-octet matrix element ($\langle 0|{}^3P_0^8|0\rangle$) should be of the order of $0.008 m_c^2$ GeV^3 or less. The constrained region is not compatible with the values of the long distance matrix elements fitted at hadron colliders.

1 Introduction

The non-relativistic quantum chromodynamics (NRQCD) [1] factorization approach is widely used to describe the production and decay of heavy quarkonium and has acquired significant achievements since it was proposed. The surplus production of J/ψ and ψ' in the large transverse momentum region at the Tevatron and the LHC seems to be powerful evidence in favor of NRQCD [2–5]. Furthermore, the complete next-to-leading order (NLO) corrections (including the contributions from the color-octet and color-singlet channels) were introduced and theoretical predictions with an identical set of long distance matrix elements (LDMEs) were almost compatible with all the J/ψ yield data at hadron colliders [6–9]. Additionally, χ_c production at hadron colliders was proved to be a successful case for the NLO NRQCD calculations [10]. For the long-pending polarization puzzle of J/ψ production, it seems also to be understood naturally using the NLO calculations [11]. Subsequently, the NLO analysis was also made for the η_c production at hadron colliders and fitted the data well using a set of compilable LDMEs with the J/ψ polarization[12,13][1].

However, there are still some puzzles. The universality problem of the LDMEs is one of the notable difficulties. The color-octet LDMEs extracted from the J/ψ yield data by the different theoretical groups were incompatible with each other. For the J/ψ polarization and η_c production, there are also different views in which NLO NRQCD calculations cannot describe the data well [14–16]. The entirely difference conclusions derive from the different selections of the LDMEs. It seems the three color-octet LDMEs ($\langle{}^3S_1^8\rangle$, $\langle{}^1S_0^8\rangle$, $\langle{}^3P_0^8\rangle$) cannot be determined independently only using the present J/ψ hadroproduction data. In the work of Chao et al. [6], they introduce two linear combinations of the three color-octet LDMEs. Only the two new LDMEs are extracted from the data and the values of χ^2 will be substantially reduced. It may imply the higher-order corrections should be considered to determine the exact magnitude of the three color-octet LDMEs. Meanwhile, the analysis combined with the data at other colliders [9] or the data of other charmonium states (e.g. η_c) [12–14] production may help to determine the magnitude of the three color-octet LDMEs.

[a] e-mail: nophy0@gmail.com
[b] e-mail: liukuiyong@lnu.edu.cn

[1] In fact, different groups adopt different strategies to fit to the data, therefore, obtained different conclusions. Chao et al. fit to the J/ψ yield production and polarization from CDF measurements. Their calculations suggest the unpolarized data could be understood by assuming that the contributions from the ${}^3S_1^8$ and ${}^3P_0^8$ channels cancel or the ${}^1S_0^8$ channel dominate the cross sections in comparison with other channels [6,7,11]. Meanwhile, η_c production at the LHC could be understood in the same theoretical framework [12]. But the referred work does not fit the HERA ep production data and cannot describe the LHC distributions. One the other hand, Butenschön et al. use the p_T distribution from the world data including the HERA data [8,9]. But the polarization cannot be explained and theoretical predictions of the cross sections for η_c production greatly overshoot the LHCb data [14].

The inclusive J/ψ production in e^+e^- annihilation is a probe to verify the color-octet mechanism and provide people with a way to place restrictions on the color-octet LDMEs. The color-octet processes in the inclusive J/ψ production associated with light hadrons involve several channels including $e^+e^- \to c\bar{c}(^3S_1^8)+q\bar{q}, e^+e^- \to c\bar{c}(^3S_1^8)+gg$ and $e^+e^- \to c\bar{c}(^1S_0^8, ^3P_J^8) + g$. At the B-factory ($\sqrt{s}$ = 10.6 GeV), the short-distance coefficients (SDCs) are negligible for the $^3S_1^8$ channels [17]. In the previous work [18], a constraint of the color-octet LDMEs ($^1S_0^8$ and $^3P_J^8$) was obtained using the data of the inclusive J/ψ production at the B-factory. Meanwhile, some data of the exclusive J/ψ production near the J/ψ mass threshold have been released [19–24]. In this paper, we attempt to revisit the constraint on the values of the color-octet LDMEs of J/ψ production and two kinds of energy region including the B-factory and also the near-threshold region will be considered in the analysis.

2 Numerical results and analysis

Under the framework of the NRQCD factorization formalism, the color-singlet channel ($^3S_1^1$) and the color-octet channels ($^3S_1^8$, $^1S_0^8$, $^3P_0^8$) can contribute the $J/\psi + X_{\text{non-}c\bar{c}}$ cross sections,

$$\sigma_{\text{non-}c\bar{c}} = \sum_n \sigma[n] = \sigma[^3S_1^1] + \sigma[^3S_1^8] + \sigma[^1S_0^8] + \sigma[^3P_0^8]. \quad (1)$$

Up to $\mathcal{O}(\alpha_s + v^2)$, the cross section for each channel can be represented as the product of the SDCs and the LDMEs,

$$\begin{aligned}\sigma[n] &= \{d^{00} + d^{10}\}\langle 0|\mathcal{O}[n]|0\rangle + d^{02}\langle 0|\mathcal{P}[n]|0\rangle \\ &= \{d^{00} + d^{10} + d^{02}m_c^2\langle v^2\rangle\}\langle 0|\mathcal{O}[n]|0\rangle \\ &\equiv \hat{\sigma}[n]\langle 0|\mathcal{O}[n]|0\rangle. \end{aligned} \quad (2)$$

Here d^{00}, d^{10}, d^{02} denote the SDCs of the order of $\alpha_s^0 v^0$, $\alpha_s^1 v^0$, $\alpha_s^0 v^2$, respectively. The above matrix element $\langle v^2\rangle$ is defined as the ratio between the NLO LDMEs in $\mathcal{O}(v^2)$ and the LO LDMEs in $\mathcal{O}(v^0)$,

$$\langle v^2\rangle \equiv \frac{\langle 0|\mathcal{P}|0\rangle}{m_c^2\langle 0|\mathcal{O}|0\rangle}. \quad (3)$$

According to the velocity scaling (power counting) rules [1], one could estimate the magnitude of this matrix element as $\langle v^2\rangle \sim v^2$. Here v is the relative velocity between the heavy quark and anti-quark in the center-of-mass frame of $Q\bar{Q}$ pair and $v^2 \approx 0.3$ for charmonium.

2.1 B-factory region

At the B-factory, the large gaps between the LO predictions and the experimental data in the exclusive and inclusive production of J/ψ have been greatly alleviated with the NLO corrections in the color-singlet frame [25–28]. It leaves little room for the color-octet mechanism. In the previous work [18], the authors gave an upper limit of the combined color-octet matrix elements ($M_k = \langle 0|\mathcal{O}(^1S_0^8)|0\rangle + k\langle 0|\mathcal{O}(^3P_0^8)|0\rangle/m_c^2$) using the NLO results in α_s and the non-$c\bar{c}$ cross sections ($\sigma^{exp.}(e^+e^- \to J/\psi + X_{\text{non-}c\bar{c}}) = (0.43 \pm 0.09 \pm 0.09)$ pb) measured by Belle [29]: $M_{4.0}^{\alpha_s} < (2.0 \pm 0.6) \times 10^{-2}$ GeV^3. In this paper, the relativistic corrections are also considered besides the radiative corrections, then the constraint will be revised as

$$\begin{cases} M_{3.8\pm1.3}^{(\alpha_s,v^2)} < (2.0 \pm 0.9) \times 10^{-2}\ \text{GeV}^3 & \mu = 2m_c, \\ M_{3.9\pm0.8}^{(\alpha_s,v^2)} < (2.5 \pm 1.0) \times 10^{-2}\ \text{GeV}^3 & \mu = \sqrt{s}/2, \end{cases} \quad (4)$$

with the following input parameters from potential model calculations [30]:

$$m_c = 1.4 \pm 0.2\ \text{GeV}, \quad \langle v^2\rangle = 0.225 \pm 0.1. \quad (5)$$

The strong-coupling constant α_s is evolved by the two-loop formula,

$$\frac{\alpha_s(\mu)}{4\pi} = \frac{1}{\beta_0 L} - \frac{\beta_1 \ln L}{\beta_0^3 L^2}, \quad (6)$$

where $L = \ln(\mu^2/\Lambda_{\text{QCD}}^2)$ with $\Lambda_{\text{QCD}} \approx 388$ MeV, $\beta_0 = (11/3)C_A - (4/3)T_f n_f$ and $\beta_1 = (34/3)C_A^2 - 4C_F T_f n_f - (20/3)C_A T_f n_f$ are the one-loop and two-loop coefficients of the QCD beta function, respectively. μ is the renormalization scale and n_f is the active quark flavors which is set to 3 for charmonium. In Eq. (4), we choose two kinds of cases for the renormalization scale as $\mu = 2m_c$ and $\mu = \sqrt{s}/2$, respectively, to show the uncertainties from renormalization scale.

In previous work [9,11,13,15,31,32], the LDMEs in J/ψ production were extracted from the experimental data of the $J/\psi/\eta_c$ hadronic production and are listed in Table 1. The differences among the numerical values reveal the difficulties to determine the exact values of the color-octet LDMEs. The work by Chao et al. implies that a wide range of values for $\langle ^1S_0^8\rangle$ can satisfy the yields and polarizations of the J/ψ production at hadron colliders [6,7,11,12]. The polarization puzzle can be understood in two different ways: the contributions from $^3P_0^8$ and $^3S_1^8$ channels (1) cancel to each other or (2) are both small. The latter way requires very small values for $\langle ^3P_0^8\rangle$ and $\langle ^3S_1^8\rangle$. The corresponding values of the combined matrix elements are also listed in the table. Most of the sets of LDMEs do not satisfy the constraint given by Eq. (4) except the set of LDMEs fitted by Butenschön et al.

Table 1 The LDMEs for J/ψ production extracted from the $J/\psi/\eta_c$ hadronic production through six works in units of 10^{-2} GeV^3 [9,11,13,15,31,32]

	$\langle 0\vert O[^1S_0^8]\vert 0\rangle$	$\frac{\langle 0\vert O[^3P_0^8]\vert 0\rangle}{m_c^2}$	$M_{3.8\pm 1.3}$
Butenschön et al. [9] without feed down	4.97 ± 0.44	-0.821 ± 0.256	1.8 ± 1.5
Butenschön et al. [9] with feed down	3.04 ± 0.35	-0.463 ± 0.156	1.3 ± 0.9
Chao et al. [11]			
Set 1	8.9 ± 0.98	0.56 ± 0.21	11.0 ± 1.5
Set 2	0	2.4	9.1 ± 3.1
Set 3	11	0	11
Gong et al. [15]	9.7 ± 0.9	-0.95 ± 0.25	6.1 ± 1.8
Bodwin et al. [31]	9.9 ± 2.2	0.56 ± 0.53	12.0 ± 3.1
Zhang et al. [13]	0.44 —1.13	1.7 ± 0.5	7.2 ± 2.9
Bodwin et al. [32]	11.0 ± 1.4	-0.312 ± 0.151	9.8 ± 1.6

2.2 Near-threshold region

Near the J/ψ mass threshold, there are no released data for the inclusive J/ψ production. Meanwhile, the BESIII and Belle collaborations measured the cross sections in the $J/\psi\pi^+\pi^-$ final states at $\sqrt{s} = 3.2-5.5$ GeV [23,24]. According to the results of their fit [23], the continuum cross sections are sightly above 5 pb and below 10 pb. The inclusive cross sections will be larger in magnitude than that of $J/\psi\pi^+\pi^-$ production by an enhancing factor. Assuming the factor is 2 at least, the numerical values of inclusive cross sections will be above 10 pb.

For the theoretical calculations, the reliable predictions cannot be obtained at the region extremely near the threshold. Therefore, in our analysis we will concentrate on the energy regions of 4.6−5.6 GeV in which the non-perturbative effects are suppressed[2]. The short-distance cross sections are shown in Table 2 and the same set of parameters in Eqs. (5, 6) are employed in the calculations. The relativistic and radiative corrections are included for the color-octet channels $^1S_0^8$ and $^3P_0^8$. For the $^3S_1^8$ and color-singlet $^3S_1^1$ channel, we give only the leading order results but one will find their numerical values are smaller in comparison with the color-octet channels even the higher-order corrections are considered. (We argue that the NLO radiative and relativistic corrections may enhance the color-singlet short-distance cross sections by a factor of about 2.2−2.3 [26,27,39].) From the table, one can see that the short-distance cross sections of $^3P_0^8$ channel are three order of magnitude larger than that of color-singlet channel. The short-distance cross sections of the $^1S_0^8$ channel are about two order of magnitude larger than that of color-singlet channel.

The total cross sections are sensitive to the selections of the color-octet LDMEs. The large SDCs shown in Table 2 imply the values of the LDMEs should be small. The negative cross sections may be obtained for the large negative P-wave LDMEs. For example, using the LDMEs fitted by Butenschön et al., the total cross sections in the energy region of 4.6−5.6 GeV will be negative. Given that the $^1S_0^8$ LDMEs are of the order of 0.1 GeV^3, the contributions from $^1S_0^8$ channel might saturate or overshoot the data.

Next, we try to give a constraint of LDMEs using the above calculations in the energy region of 4.6−5.6 GeV. As mentioned above, the numerical values of the total inclusive cross sections must be larger than that in the process of $J/\psi\pi^+\pi^-$ and should be above 10 pb as the below expression,

$$\sigma_{\text{non-}c\bar{c}} = \sigma[^1S_0^8] + \sigma[^3P_0^8] + \sigma[^3S_1^1] > 10 \text{ pb}. \tag{7}$$

Here, we neglect the contributions from $^3S_1^8$ channel which are about two order of magnitude smaller than that from $^1S_0^8$ channel referring to the SDCs shown in Table 2 and considering the $^3S_1^8$ LDMEs to be of the same order of magnitude as the $^1S_0^8$ LDMEs. In addition, the color-singlet matrix element $\langle ^3S_1^1\rangle$ is of the order of 1 GeV^3 and referring to the SDCs in Table 2, therefore the color-singlet cross sections would be less than 10 pb. According to the above discussions, we suggest a looser constraint for the color-octet LDMEs:

$$\sigma[^1S_0^8] + \sigma[^3P_0^8] > 0 \text{ pb}. \tag{8}$$

But we note that the color-singlet channels may contribute significantly to the total cross sections if the color-singlet

[2] Note that it is questionable that NRQCD could be safely applied in low energy region. Take the studies of the J/ψ production at hadron colliders as an example, the work of Chao et al., Gong et al. and Zhang et al. [6,7,11–13,15] adopts a relative large p_T cutoff as $p_T > 7$ GeV, which is over twice as large as the J/ψ mass to fit to the data. But big differences are observed between the yield data and the theoretical predictions when $p_T < 7$ GeV. In Ref. [33], the authors suggest a selection cut $p_T/M_H > 3$, required to well describe the yield data and the polarization. To solve the problem in the low p_T region, some strategies are presented such as the color glass condensate plus NRQCD method [34]. In contrast, in the works of Butenschön et al. [8,9], their fit using the p_T distributions of world data could be compatible with the J/ψ yield data. On the other hand, some works have been done in the near-threshold (BESIII) region within NRQCD factorization [35–37]. Meanwhile, some new factorization approach has been proposed to avoid the difficulties NRQCD encounters [38].

Table 2 The SDCs of different channels for J/ψ Fock states in the center-of-mass energy region of 4.6−5.6 GeV are listed in this table and denoted by $\hat{\sigma}[^{2s+1}L_J^{1,8}]$, which is defined in Eq. (2). The uncertainties of the color-octet SDCs are combined from that of m_c and $\langle v^2\rangle$. The strong-coupling constant α_s is running with the renormalization scale μ. In each cell, the number outside the bracket is evolved with $\mu = 2m_c$ and $\mu = \sqrt{s}/2$ for inside

$\sqrt{s}$ (GeV)	$\hat{\sigma}[^3S_1^1]$ (pb/GeV^3)	$\hat{\sigma}[^3S_1^8]$ (pb/GeV^3)	$\hat{\sigma}[^1S_0^8]$ (pb/GeV^3)	$m_c^2\hat{\sigma}[^3P_J^8]$ (pb/GeV^3)
4.6	3.2 (3.9)	6.0 (7.3)	$462.3^{+224.4}_{-160.1}$ ($520.4^{+186.1}_{-153.1}$)	$6376.9^{+1732.2}_{-563.3}$ ($7151.0^{+2602.6}_{-1182.4}$)
4.8	2.8 (3.2)	5.2 (6.0)	$405.7^{+222.1}_{-132.0}$ ($443.9^{+184.7}_{-121.5}$)	$4794.8^{+989.3}_{-254.4}$ ($5235.0^{+1533.2}_{-646.6}$)
5.2	2.2 (2.4)	4.3 (4.6)	$312.9^{+132.4}_{-91.9}$ ($326.1^{+99.9}_{-79.0}$)	$2898.4^{+340.0}_{-55.6}$ ($3018.6^{+591.6}_{-244.7}$)
5.4	2.1 (2.1)	4.1 (4.2)	$275.5^{+112.7}_{-78.8}$ ($281.0^{+82.8}_{-66.2}$)	$2314.0^{+187.5}_{-45.6}$ ($2359.7^{+367.1}_{-143.3}$)
5.6	1.9 (1.9)	3.9 (3.9)	$257.1^{+82.7}_{-81.1}$ ($257.1^{+55.6}_{-68.8}$)	$1975.8^{+42.9}_{-100.7}$ ($1975.8^{+136.3}_{-177.8}$)

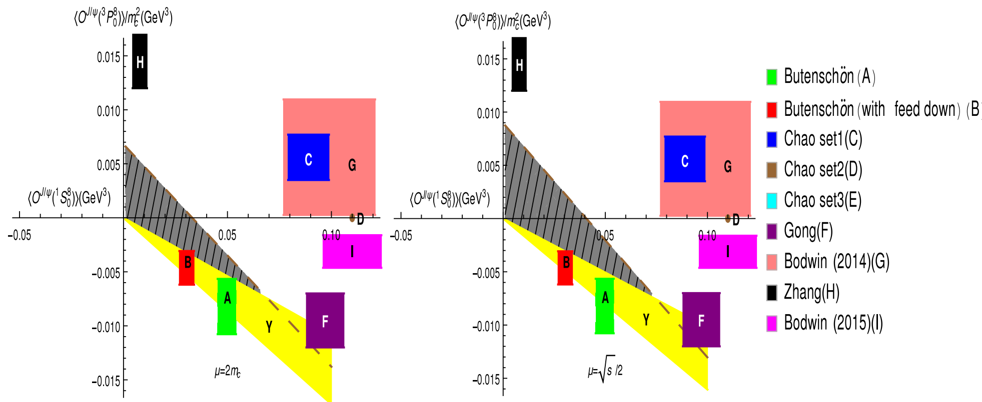

Fig. 1 The constraints of LDMEs are given using the experimental data of J/ψ inclusive production at the B-factory [29] and $J/\psi\pi^+\pi^-$ production in the energy region of 4.6−5.6 GeV [23,24]. The former gives an upper bound corresponding to the *brown dashed line*. The latter gives a lower bound corresponding to the *yellow band labeled Y*. The *gray shaded region* presents the combined constraints to LDMEs. For comparison, the LDMEs extracted from the fit to the hadron colliders data in Table 1 are also shown and correspond to areas labeled *A* to *I*. The LDMEs of "Chao set3" which exceed the display range are not given in the plot

LDME is one or two orders of magnitude larger than the color-octet LDMEs.

The results of the constraint are shown in Fig. 1. Using the SDCs in Table 2, a lower bound curve will be obtained for each distinct center-of-mass energy according to Eq. (8). Subsequently, the extreme curves form the edges of the yellow band labeled Y. The LDMEs should be restricted above all the curves, therefore, above the yellow band labeled Y. The gray shaded region shows the constraints to LDMEs combined the data at the B-factory and in the energy region of 4.6−5.6 GeV. As shown in Fig. 1, almost all the LDMEs fitted at hadron colliders are incompatible with the constraints. It leads to challenges to the universality of the NRQCD LDMEs. The dependence of the renormalization scale can be seen in the figure in which both the cases with $\mu = 2m_c$ and with $\mu = \sqrt{s}/2$ are given. In comparison with the lower bound derived from the near-threshold data, the upper bound from the B-factory data seems to heavily depend on the renormalization scale. The LDMEs are restricted to an extremely small area. In practice, the P-wave LDMEs $\langle^3P_0^8\rangle$ are restricted to the region of about $-0.008m_c^2$ to $0.009m_c^2$ GeV^3. Note that the inclusive data observed by the Belle and BaBar is not compatible with each other: the total prompt J/ψ cross sections measured by BaBar [40] are twice as large as the values measured by Belle [29]. Therefore, further clarification is needed and the upper bound of the constraint region would make changes accordingly.

3 Summary

In this paper, we extend the previous work in Ref. [18] and study the color-octet LDMEs ($\langle^1S_0^8\rangle$, $\langle^3P_0^8\rangle$) in inclusive J/ψ production at e^+e^- colliders. Both the radiative and the relativistic corrections are considered within the NRQCD framework. An upper bound of the LDMEs is obtained using the data at the B-factory. According to the released data of the exclusive J/ψ production associated with $\pi^+\pi^-$ in the energy region of 3.2−5.5 GeV, we argue that the color-octet cross sections of the inclusive J/ψ production must be larger in magnitude than zero picobarn in the region of 4.6−5.6 GeV and a lower bound of the LDMEs is obtained. Through our estimation, the P-wave color-octet matrix element for J/ψ ($\langle 0|^3P_0^8|0\rangle$) should be of the order of $0.008m_c^2$ GeV^3 or less.

Acknowledgements The authors would like to thank Professor K.T. Chao, C. Meng and Y.Q. Ma for useful discussion. This work was supported by the National Natural Science Foundation of China (Grants No. 11375021, No. 11447018, No. 11722539 and No. 11705078), the New Century Excellent Talents in University (NCET) under grant NCET-13-0030, the Major State Basic Research Development Program of China (No. 2015CB856701), and General project of Liaoning Provincial Education Department (No. L2015197).

References

1. G.T. Bodwin, E. Braaten, G.P. Lepage, Phys. Rev. D **51**, 1125 (1995). arXiv:hep-ph/9407339
2. T. Affolder et al., CDF Collaboration, Phys. Rev. Lett. **85**, 2886 (2000). arXiv:hep-ex/0004027
3. F. Abe et al., CDF Collaboration, Phys. Rev. Lett. **79**, 572 (1997)
4. R. Aaij et al., LHCb, Eur. Phys. J. C **73**, 2631 (2013). arXiv:1307.6379
5. S. Chatrchyan et al., CMS, Phys. Lett. B **727**, 381 (2013). arXiv:1307.6070
6. Y.-Q. Ma, K. Wang, K.-T. Chao, Phys. Rev. Lett. **106**, 042002 (2011). arXiv:1009.3655
7. Y.-Q. Ma, K. Wang, K.-T. Chao, Phys. Rev. D **84**, 114001 (2011). arXiv:1012.1030
8. M. Butenschön, B.A. Kniehl, Phys. Rev. Lett. **106**, 022003 (2011). arXiv:1009.5662
9. M. Butenschön, B.A. Kniehl, Phys. Rev. D **84**, 051501 (2011). arXiv:1105.0820
10. Y.-Q. Ma, K. Wang, K.-T. Chao, Phys. Rev. D **83**, 111503 (2011). arXiv:1002.3987
11. K.-T. Chao, Y.-Q. Ma, H.-S. Shao, K. Wang, Y.-J. Zhang, Phys. Rev. Lett. **108**, 242004 (2012). arXiv:1201.2675
12. H. Han, Y.-Q. Ma, C. Meng, H.-S. Shao, K.-T. Chao, Phys. Rev. Lett. **114**, 092005 (2015). arXiv:1411.7350
13. H.-F. Zhang, Z. Sun, W.-L. Sang, R. Li, Phys. Rev. Lett. **114**, 092006 (2015). arXiv:1412.0508
14. M. Butenschön, Z.-G. He, B.A. Kniehl, Phys. Rev. Lett. **114**, 092004 (2015). arXiv:1411.5287
15. B. Gong, L.-P. Wan, J.-X. Wang, H.-F. Zhang, Phys. Rev. Lett. **110**, 042002 (2013). arXiv:1205.6682
16. M. Butenschön, B.A. Kniehl, Phys. Rev. Lett. **108**, 172002 (2012). arXiv:1201.1872
17. F. Yuan, C.-F. Qiao, K.-T. Chao, Phys. Rev. D **56**, 321 (1997). arXiv:hep-ph/9703438
18. Y.-J. Zhang, Y.-Q. Ma, K. Wang, K.-T. Chao, Phys. Rev. D **81**, 034015 (2010). arXiv:0911.2166
19. M. Ablikim et al. (BESIII), Phys. Rev. Lett. **118**, 092001 (2017). arXiv:1611.01317
20. C.P. Shen et al., Belle. Phys. Rev. D **89**, 072015 (2014). arXiv:1402.6578
21. M. Ablikim et al. (BESIII), Phys. Rev. D **91**, 112005 (2015). arXiv:1503.06644
22. M. Ablikim et al. (BESIII), Phys. Rev. D **94**, 032009 (2016). arXiv:1605.03256
23. Z. Liu et al., Belle Collaboration, Phys. Rev. Lett. **110**, 252002 (2013). arXiv:1304.0121
24. M. Ablikim et al., BESIII, Phys. Rev. Lett. **110**, 252001 (2013). arXiv:1303.5949
25. B. Gong, J.-X. Wang, Phys. Rev. D **80**, 054015 (2009). arXiv:0904.1103
26. B. Gong, J.-X. Wang, Phys. Rev. Lett. **102**, 162003 (2009). arXiv:0901.0117
27. Y.-Q. Ma, Y.-J. Zhang, K.-T. Chao, Phys. Rev. Lett. **102**, 162002 (2009). arXiv:0812.5106
28. Y.-J. Zhang, Y.-J. Gao, K.-T. Chao, Phys. Rev. Lett. **96**, 092001 (2006). arXiv:hep-ph/0506076
29. P. Pakhlov et al., Belle Collaboration, Phys. Rev. D **79**, 071101 (2009). arXiv:0901.2775
30. G.T. Bodwin, H.S. Chung, D. Kang, J. Lee, C. Yu, Phys. Rev. D **77**, 094017 (2008). arXiv:0710.0994
31. G.T. Bodwin, H.S. Chung, U.-R. Kim, J. Lee, Phys. Rev. Lett. **113**, 022001 (2014). arXiv:1403.3612
32. G.T. Bodwin, K.-T. Chao, H.S. Chung, U.-R. Kim, J. Lee, Y.-Q. Ma, Phys. Rev. D **93**, 034041 (2016). arXiv:1509.07904
33. P. Faccioli, V. Knünz, C. Lourenco, J. Seixas, H.K. Wöhri, Phys. Lett. B **736**, 98 (2014). arXiv:1403.3970
34. Y.-Q. Ma, R. Venugopalan, Phys. Rev. Lett. **113**, 192301 (2014). arXiv:1408.4075
35. K.-T. Chao, Z.-G. He, D. Li, C. Meng (2013). arXiv:1310.8597
36. Y.-J. Li, G.-Z. Xu, K.-Y. Liu, Y.-J. Zhang, JHEP **1401**, 022 (2014). arXiv:1310.0374
37. G.-Z. Xu, Y.-J. Li, K.-Y. Liu, Y.-J. Zhang, JHEP **1410**, 71 (2014). arXiv:1407.3783
38. Y.-Q. Ma, K.-T. Chao (2017). arXiv:1703.08402
39. Z.-G. He, Y. Fan, K.-T. Chao, Phys. Rev. D **81**, 054036 (2010). arXiv:0910.3636
40. B. Aubert et al., BABAR, Phys. Rev. Lett. **87**, 162002 (2001). arXiv:hep-ex/0106044